Characterizing interactions in fine magnetic particle systems using first order reversal curves

Christopher R. Pike[a)]
Department of Geology, University of California, Davis, California 95616

Andrew P. Roberts
Department of Oceanography, University of Southampton, Southampton Oceanography Centre, European Way, Southampton SO14 3ZH, United Kingdom

Kenneth L. Verosub
Department of Geology, University of California, Davis, California 95616

(Received 1 June 1998; accepted for publication 1 February 1999)

We demonstrate a powerful and practical method of characterizing interactions in fine magnetic particle systems utilizing a class of hysteresis curves known as first order reversal curves. This method is tested on samples of highly dispersed magnetic particles, where it leads to a more detailed understanding of interactions than has previously been possible. In a quantitative comparison between this method and the δM method, which is based on the Wohlfarth relation, our method provides a more precise measure of the strength of the interactions. Our method also has the advantage that it can be used to decouple the effects of the mean interaction field from the effects of local interaction field variance. © *1999 American Institute of Physics.* [S0021-8979(99)08309-7]

I. INTRODUCTION

Magnetic interactions between particles are a major determinant of noise levels in magnetic recording media. The conventional methods[1–3] of characterizing magnetic interactions utilize isothermal remanent magnetization (IRM) and dc demagnetization remanence (DCD) curves, and are based on the Wohlfarth[4] relation. The most important among these methods is the δM method.[5,6] In this paper, an alternative approach is described which employs first order reversal curves (FORCs).[7] A typical set of FORCs is shown in Fig. 1. The structure present in this set of curves is not readily apparent, but it can be emphasized with a mixed second derivative as described more formally below. In this fashion, the FORCs of Fig. 1 can be transformed into the contour plot of Fig. 2, which we will refer to as a FORC diagram. (There are obvious similarities between a FORC diagram and a Preisach diagram,[8] but there are also important distinctions, which we discuss in Appendix A.)

We have developed a practical technique for measuring and calculating accurate FORC diagrams. This technique requires thousands of data points, and, until recently, would have been impractical. However, with the advent of a commercially available, automated alternating field gradient magnetometer,[9] the acquisition of a FORC diagram is a straightforward task, requiring only a couple of hours for data collection and analysis.

II. EVALUATION OF A FORC DIAGRAM

The measurement of a FORC, as shown in Fig. 3, begins with the saturation of the sample by a large positive applied field. This field is ramped down to a reversal field H_a. The FORC consists of a measurement of the magnetization as the field is then increased from H_a back up to saturation. The magnetization at applied field H_b on the FORC with reversal point H_a is denoted by $M(H_a,H_b)$, where $H_b \geqslant H_a$. A FORC distribution is defined as the mixed second derivative:

$$\rho(H_a,H_b) \equiv -\frac{\partial^2 M(H_a,H_b)}{\partial H_a \partial H_b}, \tag{1}$$

where this is well defined only for $H_b > H_a$.

When a FORC distribution is plotted, it is convenient to change coordinates from $\{H_a,H_b\}$ to $\{H_c \equiv (H_b - H_a)/2, H_u \equiv (H_a + H_b)/2\}$. A FORC diagram is a contour plot of a FORC distribution with H_c and H_u on the horizontal and vertical axes, respectively. Since $H_b > H_a$, then $H_c > 0$, and a FORC diagram is confined to the right side half plane. As shown below, when the basic Preisach model is used, H_c is equivalent to a particle coercivity and H_u to a local interaction field.

To evaluate a FORC diagram, first the boundaries of the desired diagram in the H_c, H_u plane are selected. The reversal field of the first FORC, H_{a1}, is calculated from the coordinates of the upper left corner of the diagram [i.e., $H_a = (H_u - H_c)$]; the reversal field of the last FORC, H_{aN}, is calculated from the bottom right corner; and N FORCs are measured with evenly spaced reversal fields between and including H_{a1} and H_{aN}. The data points on each individual FORC are measured with this same field spacing. The same averaging time is used in the measurement of every data point. In choosing N, the number of FORCs to be measured, there is a tradeoff between the resolution of the FORC diagram and data acquisition time. We have found that $N = 99$

a)Electronic mail: pike@geology.ucdavis.edu

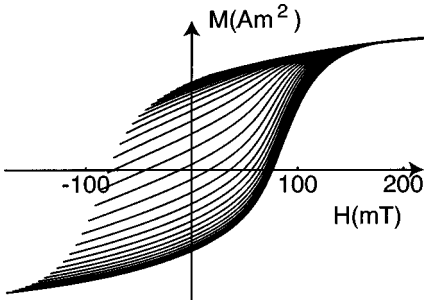

FIG. 1. A set of first order reversal curves (FORCs) for a piece of a typical floppy magnetic recording disk.

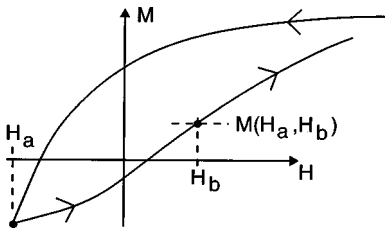

FIG. 3. Definition of a FORC. The measurement of a FORC begins with the saturation of the sample by a large positive field. This field is ramped down to a reversal field H_a. The FORC consists of a measurement of the magnetization as the field is then increased from H_a back up to saturation. The magnetization at H_b on the FORC with reversal point H_a is denoted by $M(H_a,H_b)$.

yields a reasonable resolution in an acquisition time between 1 and 2 h.

To calculate $\rho(H_a,H_b)$ we use consecutive data points from consecutive reversal curves in an array such as that shown in Fig. 4. We fit the magnetization at these points with a polynomial surface of the form: $a_1+a_2H_a+a_3H_a^2+a_4H_b+a_5H_b^2+a_6H_aH_b$; then $-a_6$ is taken as the value of $\rho(H_a,H_b)$ at the center of the array. The number of data points contained in this array is $(2*\mathrm{SF}+1)^2$, where SF is referred to as the ''smoothing factor'' and can be set between 3 for a well-behaved sample and 10 for a noisy sample. Numerical effects inevitably smooth out somewhat the features of a FORC distribution; the degree of smoothing increases with the value of SF. In practice, one tries to use the smallest value of SF possible, while keeping noise on a FORC diagram to acceptable levels. The FORC diagrams in this paper were evaluated with SF=3.

III. EXPERIMENTAL RESULTS

FORC distributions were measured for a sample of magnetic recording material from a typical floppy disk and for samples of highly dispersed, single domain magnetic particles prepared by Eastman Kodak Company Research Laboratories at four concentrations of: 1.5%, 3%, 6% and 9% of magnetic material by mass. As far as it was possible to control, the concentration of particles and, hence, the proximity of particles to each other, was the only parameter allowed to vary between samples.

FORC diagrams for the floppy disk material and for a 1.5% Kodak sample are shown in Figs. 2 and 5, respectively. The averaging time spend at each data point was 0.4 s. To emphasize the differences between the Kodak samples, we also acquired FORC diagrams for a smaller region of the FORC plane, as shown in Fig. 6 for a 1.5% and 9% sample. Each FORC diagram required a separate measurement of 99 FORCs. Since the diagrams in Fig. 6 have a smaller size, the 99 FORCs used to evaluate them had a smaller field spacing (1 mT) than those used to calculate Fig. 5 (2 mT), which provides for a greater resolution.

IV. THEORETICAL MODELS

A FORC diagram contains a large amount of information, but this information is of little use if it cannot be correctly interpreted. To facilitate our interpretation of these diagrams, we can study the FORC diagrams associated with theoretical models. This will permit us to assign interpretations to the features we see on experimental diagrams. Therefore, below we calculate FORC distributions for some simple theoretical models.

A. Noninteracting single domain particles

Our first model consists of a collection of noninteracting single domain, particles. The magnetic behavior of an individual single domain particle can, to a good approximation, be represented as the sum of a reversible component and a square hysteresis loop. In the noninteracting case, the reversible component will vanish when the second derivative in Eq. (1) is taken and can be ignored. The half width of the square loop is termed a particle's switching field. A collection of particles can be represented by a distribution of switching fields $f(H_{\mathrm{sw}};H_{\mathrm{sw}}>0)$, where $\int_0^\infty dx\, f(x)=1$. To

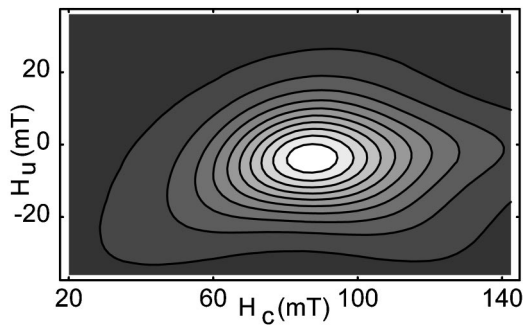

FIG. 2. A FORC diagram for a floppy disk sample. Calculated from 99 FORCs of which the data in Fig. 1 are a subset.

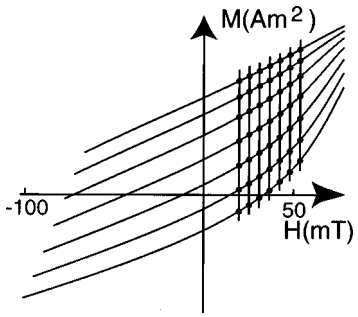

FIG. 4. A subset of seven consecutive FORCs from Fig. 1. The circled points are a 7×7 array of data points evenly spaced in H_a and H_b.

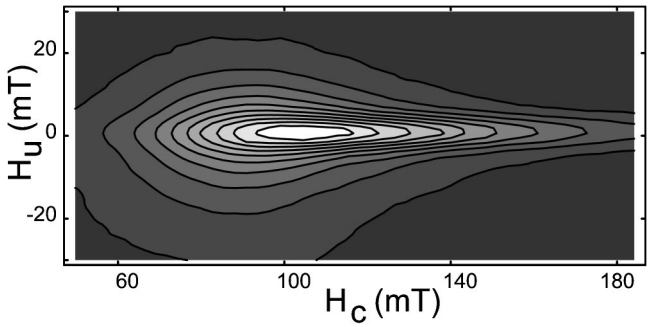

FIG. 5. FORC diagram for a 1.5% Kodak sample. Field spacing: 3 mT.

calculate the magnetization on a FORC, we start with a saturating positive applied field, so all the particles have a positive orientation. At H_a, particles with switching fields in the range $0 \leqslant H_{sw} \leqslant -H_a$ have switched to negative; when the field is increased to H_b, particles in the range $H_b < H_{sw} \leqslant -H_a$ will remain negative. Thus, $M(H_a, H_b)$ can be written

$$M(H_a, H_b) = 1 - 2 \int_{\mathrm{Max}[0, H_b, -H_a]}^{\mathrm{Max}[0, -H_a]} dH_{sw} f(H_{sw}). \tag{2}$$

The first derivative of $M(H_a, H_b)$ with respect to H_b is:

$$dM(H_a, H_b)/dH_b = 2 f(H_b) \quad \text{for } 0 < H_b \leqslant -H_a,$$
$$= 0 \quad \text{for } -H_a < H_b,$$

which can be written as

$$dM(H_a, H_b)/dH_b = 2 f(H_b) \theta(-H_a - H_b) \theta(H_b), \tag{3}$$

where $\theta(x)$ is the step function which equals 0 for $x < 0$ and 1 for $x \geqslant 0$. The derivative of $\theta(x)$ is $\delta(x)$, where $\delta(x)$ is a delta function. The derivative of Eq. (3) with respect to H_a is

$$\rho(H_a, H_b) \equiv -\frac{\partial^2 M(H_a, H_b)}{\partial H_a \partial H_b} = 2 f(H_b) \delta(H_a + H_b) \theta(H_b). \tag{4}$$

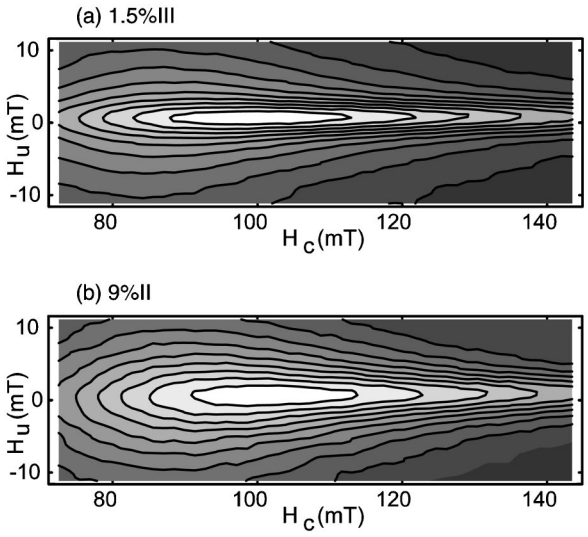

FIG. 6. FORC diagram for: (a) 1.5% and (b) 9% Kodak samples. Field spacing: 1 mT.

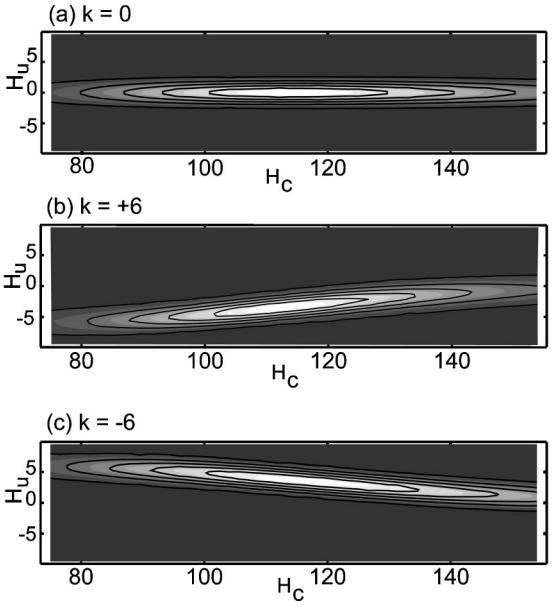

FIG. 7. FORC diagrams for a system of single domain particles in three models: (a) noninteracting model; (b) mean interaction field model with $k = +6$, and (c) mean interaction field model with $k = -6$ ($\mu_{sw} = 120$ and $\sigma_{sw} = 0.4$).

Changing coordinates, we get $\rho(H_c, H_u) = 2 f(H_c) \delta(H_u) \theta(H_c)$. Hence, this theoretical $\rho(H_c, H_u)$ is a positive-valued delta function located on the $H_u = 0$ axis, for $H_c > 0$.

To illustrate the properties of this model, we used Eq. (2) to calculate points on 99 FORCs, and from this set of theoretical FORC data we calculated the FORC diagram shown in Fig. 7(a). A lognormal function was used for $f(H_{sw})$ with a logarithmic mean[10] $\mu_{sw} = 120$ and a logarithmic variance[10] $\sigma_{sw} = 0.4$. The distribution in Fig. 7(a) is highly peaked on the $H_u = 0$ axis, which is characteristic of a noninteracting system. The small vertical spread that is present can be attributed to numerical smoothing effects. In an experimental measurement of a FORC distribution, some vertical spread will always be present due to numerical effects, even in the absence of interactions. However, as we will show, the FORC distribution of a real sample with interactions (e.g., Fig. 2) will have a greater spread than can be attributed to numerical smoothing alone.

B. Single domain particles with interactions: The basic Preisach model

There does not exist an accurate physical model of interacting magnetic particles that is practical for calculations. However, as a simplification, the above-described model can be combined with a local interaction field which is assumed to be constant at a given particle site but which varies randomly from site to site. This interaction field is also assumed to be aligned with the applied field. The distribution of interaction field values is denoted by $g(H_{int})$, where g is symmetric about $H_{int} = 0$ and $\int_{-\infty}^{\infty} dH_{int}\, g(H_{int}) = 1$. It is also as-

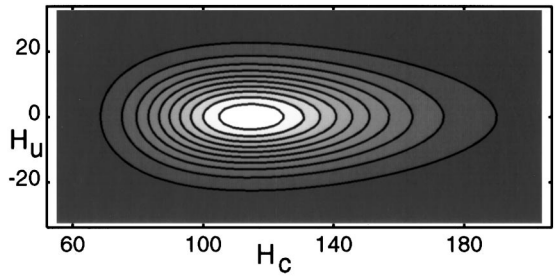

FIG. 8. FORC diagram for a system of interacting single domain particles modeled with the basic Preisach model ($\mu_{sw}=120$, $\sigma_{sw}=0.4$, and $\sigma_{int}=9$).

sumed that there is no correlation between the switching field and the interaction field: This model has been referred to as the basic Preisach model.

Again, all particles begin in a positive orientation. At H_a, particles for which $H_a+H_{int}<-H_{sw}$ have switched to negative [this can be written: $H_{int}<-(H_{sw}+H_a)$]. At H_b, particles for which $(H_b+H_{int})<H_{sw}$ will remain switched [giving $H_{int}<(H_{sw}-H_b)$]. In summary, a particle will have a negative orientation at H_b if H_{int} satisfies both of these inequalities, that is: $H_{int}<\mathrm{Min}[-(H_{sw}+H_a),(H_{sw}-H_b)]$. Thus,

$$M(H_a,H_b)=1-2\int_0^{\infty} dH_{sw}\, f(H_{sw}) \times \int_{-\infty}^{\mathrm{Min}[-(H_{sw}+H_a),(H_{sw}-H_b)]} dH_{int}\, g(H_{int}). \quad (5)$$

Using the same approach described in Sec. IV A, and using Eq. (5) for $M(H_a,H_b)$, it can be show that $\rho(H_c,H_u)=2\,f(H_c)g(H_u)$. Hence, in the basic Preisach model, a FORC distribution $\rho(H_c,H_u)$ is equivalent to the distribution of particles $f(H_{sw})g(H_{int})$ through a simple mapping of H_c to H_{sw}, and H_u to H_{int}. The vertical spread on the FORC diagram is a manifestation of the variance in the distribution of interaction fields [i.e., $g(H_u)$].

Ninety-nine FORCs were calculated using Eq. (5) to obtain Fig. 8. We used the same lognormal distribution $f(H_{sw})$ as above, and a normal distribution for $g(H_{int})$, with standard deviation $\sigma_{int}=9.0$. The large vertical spread in Fig. 8, as compared with Fig. 7(a), is due to the presence of a randomly varying local interaction field.

C. Single domain particles with interactions: The mean field model

To examine a different type of complexity, a mean interaction field kM was added to the noninteracting model. If the magnetization on the upper (descending) half of the major hysteresis loop is denoted by $M(H_a)$, then $M(H_a)$ is given by the implicit integral

$$M(H_a)=1-2\int_0^{\mathrm{Max}\{0,-[H_a+kM(H_a)]\}} dH_{sw} f(H_{sw}), \quad (6)$$

and $M(H_a,H_b)$ on a FORC is given by

$$M(H_a,H_b)=1-2\int_{\mathrm{Max}\{0,[H_b+kM(H_a,H_b),-(H_a+kM(H_a))]\}}^{\mathrm{Max}\{0,-[H_a+kM(H_a)]\}} dH_{sw} f(H_{sw}). \quad (7)$$

Using the same $f(H_{sw})$, FORC diagrams were calculated for $k=+6$ and -6 [Figs. 7(b) and 7(c)]. Addition of a mean field has two effects. First, the peak of the distribution is displaced off the $H_u=0$ axis: the displacement is down for positive k and up for negative k. Second, the direction of contour elongation now has a positive slope for positive values of k, and a negative slope for negative values of k. However, the mean field does not increase the vertical spread of the distribution. It is therefore possible to distinguish the effect of a mean interaction field from that of local interaction field variance, which was modeled by the basic Preisach model.

In a mean field model, the reversible component of the magnetization can no longer be ignored. If $q(H)$ denotes the reversible magnetization in the absence of interactions, then the term $q(H+kM)$ should be added to the right hand side of Eqs. (6) and (7). We repeated our calculations using a realistic reversible component: $q(H)=\mathrm{ArcTan}(H/1200)/(\pi/2)$. It appears that the effect of a reversible component is to shift the peak location slightly to the left on a FORC diagram. The statements made above regarding the model's results remain valid with this shift.

D. Single domain particles with interactions: The moving Preisach model

We next combine the basic Preisach model with a mean interaction field; this has been referred to as the moving Preisach model.[11] $M(H_a)$ is given by the implicit integral:

$$M(H_a)=1-2\int_0^{\infty} dH_{sw}\, f(H_{sw}) \times \int_{-\infty}^{-[H_{sw}+H_a+kM(H_a)]} dH_{int}\, f(H_{int}), \quad (8)$$

and $M(H_a,H_b)$ is given by

$$M(H_a,H_b)=1-2\int_0^{\infty} dH_{sw}\, f(H_{sw}) \times \int_{-\infty}^{\mathrm{Min}\{-[H_{sw}+H_a+kM(H_a)],H_{sw}-H_b-kM(H_a,H_b)\}} \times dH_{int}\, g(H_{int}). \quad (9)$$

Using the same distribution functions as above, a FORC diagram was evaluated for $k=+6$ (Fig. 9). The introduction of a mean field has moved the peak of the distribution in Fig. 9 below the $H_u=0$ axis and has given the direction of contour elongation a positive slope, in agreement with the results for the above-described mean field model [see Fig. 7(b)]. Note that a dark region, which represents negative values, occurs at the bottom of Fig. 9. The presence of negative values for $\rho(H_c,H_u)$ may be surprising, but there is no mathematical reason why they are prohibited. In the basic Preisach model,

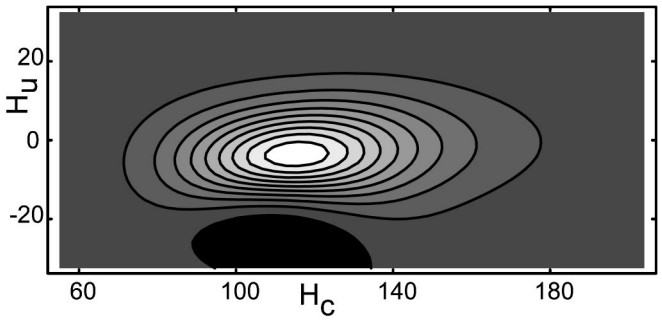

FIG. 9. FORC diagram for a system of interacting single domain particles modeled by the moving Preisach model with $k=+6$ ($\mu_{sw}=120$, $\sigma_{sw}=0.4$, and $\sigma_{int}=9$).

the distribution of particles $\rho(H_c,H_u)$ is related to $f(H_{sw})g(H_{int})$ through a one-to-one mapping of H_c to H_{sw}, and H_u to H_{int}. In this case, negative values of $\rho(H_c,H_u)$ cannot occur. However, in the moving Preisach model, the relationship is no longer a one-to-one mapping; rather, $\rho(H_c,H_u)$ is a nonlocal function of $f(H_{sw})g(H_{int})$ that can take negative values even though $f(H_{sw})g(H_{int})$ is always positive. Detailed measurements have, in fact, shown that negative values occur in the FORC distribution of the floppy disk below and to the left of the region shown in Fig. 2.

Finally, we have repeated our moving Preisach model calculation with the addition of the same reversible component described earlier. Again, the primary effect is a slight shift of the distribution peak to the left. The statements made above remain valid in the presence of this shift.

V. COMPARISON OF THEORY AND EXPERIMENT

These simplified models provide us with a framework which can be used to interpret the FORC diagrams of real samples. As we have shown, a vertical spread of the contours indicates the presence of a randomly varying local interaction field. The displacement of the distribution peak below the $H_u=0$ axis and a positive slope of the line of contour elongation are both indicative of a positive mean interaction field. Based on these criteria, we can infer that in the floppy disk sample a substantial random local field and positive mean field are present (Fig. 2).

To test these interpretations, we define the following quantitative characterizations of FORC distributions: Peak H_c and Peak H_u denote the coordinates of the distribution peak. $H_m(H_c)$ denotes a curve passing through the distribution maximum at each H_c coordinate; dH_m/dH_c denotes the slope of this curve at the distribution peak. $\rho_{1/2}$ denotes the half width of the distribution peak on a vertical cross section passing through $H_c=$ Peak H_c.

Values for the floppy and Kodak samples are compared in Table I. The half width of the FORC distributions was smallest for the 1.5% Kodak sample, as would be expected for a highly dispersed particle system. The half width is 29% greater for the 9% Kodak sample and 91% larger for the floppy disk. To enable a more accurate comparison between the Kodak samples, we have used higher resolution FORC diagrams of the type shown in Fig. 6 to define an additional measure of vertical spread:

$$\Delta H_u \equiv \frac{\iint_R dH_c dH_u \frac{2\,\mathrm{Abs}[H_u]}{hgt}\rho[H_c,H_u-H_m(H_c)]}{\iint_R dH_c dH_u\,\rho[H_c,H_u-H_m(H_c)]}, \qquad (10)$$

where R is the rectangular region encompassed by Fig. 6 (i.e., 71.6 mT$\leqslant H_c \leqslant$144.5 mT, $-12.15\leqslant H_u\leqslant$12.15 mT) and where hgt is the vertical height of the region R [i.e., hgt $=$24.3 mT]. Defined in this fashion, ΔH_u will equal 0 for a delta function and 1 for a function that is uniformly distributed on the H_u axis. A highly consistent progression of increasing ΔH_u with increasing particle concentration is observed (Table I), in agreement with our theoretical models.

The slope of the line of contour elongation dH_m/dH_c is greatest for the floppy disk, which indicates a stronger mean interaction field in this sample. dH_m/dH_c values for the Kodak samples increased consistently, for the most part, with increasing concentration. These findings confirm the validity of the above-described theoretical framework in interpreting experimental FORC data.

The Peak H_u values for the Kodak samples (Table I) are more difficult to understand. The mean interaction field model indicates that a positive mean field should result in a displacement of the distribution peak below the $H_u=0$ axis giving a negative Peak H_u, as was true for the floppy disk (Fig. 2). However, the peaks of the Kodak samples are displaced slightly above the $H_u=0$ axis (Fig. 6), giving a positive Peak H_u. This may occur because during a FORC measurement, more time is spent at the reversal point (H_a in Fig. 3) than at any of the subsequent points on a FORC. Due to magnetic viscosity effects, the additional time spent here is equivalent to a slight negative shift in the effective value of H_a, which leads to a small upward offset of the FORC distribution. This effect is quite small, but because the mean interaction field in the Kodak samples is also small, it be-

TABLE I. Measurements obtained with FORC distributions and δM_p.

Sample	Peak H_c[a] (mT)	Peak H_u[b] (mT)	dH_m/dH_c[c]	$\rho_{1/2}$ (mT)[d]	ΔH_u[e]	ΔM_p[f]
floppy	87.5	−4.0	0.061	20.2	⋯	0.295
1.5 I	100.0	0.687	0.00692	⋯	0.7187	0.216
1.5 II	99.3	0.636	0.00767	10.6	0.7133	0.214
1.5 III	99.2	0.636	0.00711	⋯	0.7178	0.215
3.0 I	103.2	0.648	0.00894	⋯	0.738	0.220
3.0 II	103.7	0.638	0.00890	⋯	0.7359	0.222
3.0 III	102.1	0.641	0.00869	⋯	0.7385	0.216
6.0 I	102.5	0.609	0.0119	⋯	0.7751	0.228
6.0 II	102.4	0.609	0.0110	⋯	0.7692	0.228
6.0 III	100.7	0.571	0.0126	⋯	0.7741	0.227
9.0 II	101.0	0.579	0.0120	13.7	0.7827	0.231
9.0 III	101.5	0.501	0.0154	⋯	0.7811	0.231

[a]Peak H_c is the H_c coordinate of the distribution peak.
[b]Peak H_u is the H_u coordinate of the distribution peak.
[c]dH_m/dH_c is the slope of $H_m(H_c)$ at the distribution peak, where $H_m(H_c)$ is a curve passing through the maximum value of the distribution at each H_c coordinate.
[d]$\rho_{1/2}$ is the half width of the distribution in a cross section through $H_c=$ Peak H_c.
[e]ΔH_u calculated with Eq. (10).
[f]δM_p is the magnitude of the negative $\delta M(H)$ peak.

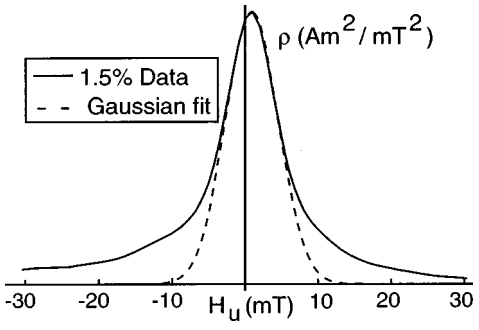

FIG. 10. Cross section of the FORC distribution of a 1.5% Kodak sample, evaluated at $H_c = 106.6$ mT.

comes observable. This hypothesis has been verified by intentionally adding a 9 s pause at the reversal point. This pause produces a further upward shift in the FORC distribution. It appears, therefore, that our experimental FORC distributions have a small, but systematic upward offset. However, increasing particle concentration should still push the H_u coordinate of the distribution peak downward, and this is observed experimentally (Table I). The fact that the distribution peak for the floppy disk (Fig. 2) is displaced below the $H_u = 0$ axis indicates that interactions in this material have completely overcome the small upward displacement due to viscosity effects.

Closer analysis of FORC diagrams makes possible a more detailed characterization of interactions in the highly dispersed Kodak samples. The inner contour loops of the Kodak FORC diagrams, in particular the 1.5% sample [Fig. 6(a)], are highly elongated in the horizontal direction. Comparison with the noninteracting model [Fig. 7(a)] suggests that these samples contain a large fraction of isolated, nearly noninteracting particles. In Fig. 10, a vertical cross section through the peak of 1.5% Kodak sample FORC distribution is plotted. The cross section is strongly peaked near the $H_u = 0$ axis. The narrow width of this peak and its proximity to the $H_u = 0$ axis indicate that a large fraction of the particles are unaffected by interactions, as would be expected for a highly dispersed sample. The small positive offset of the peak in Fig. 10 is probably due to the above-described viscosity effects.

Examination of the overall FORC distribution of the 1.5% Kodak sample indicates that while the inner contours [Fig. 6(a)] are extremely narrow, the outer contour loops (Fig. 5) are more spread out vertically. This contrasts with the basic Preisach model (Fig. 8) where the inner and outer contours have the same shape, and the floppy disk sample (Fig. 2) where all the contours have roughly the same proportions. The cross section in Fig. 10 enables a better understanding of why the outer contours in Fig. 5 have this increased vertical spread. The basic Preisach model assumes a Gaussian distribution of interaction fields, however, the cross-sectional distribution shown in Fig. 10 is not consistent with a Gaussian distribution. The distribution in Fig. 10 can be better described as the sum of a narrow and a wide Gaussian distribution. This observation suggests that these highly dispersed samples consist of two somewhat distinct populations of particles: a population of well-isolated particles, which produce the narrow Gaussian distribution, and a population of small particle clusters (perhaps couplets or triplets). Within these clusters, there is a strong, but localized, interaction which produces the wider Gaussian distribution.

Another feature of the Kodak sample FORC diagrams demonstrates a weakness of the Preisach model. Let us define the median point of a contour loop as the intersection of a vertical line that crosses the loop where its vertical spread is greatest, and a horizontal line that crosses the loop where its horizontal spread is greatest. For the Preisach model (Fig. 8), the median points coincide; we can say the contours are concentric. This is a consequence of the fact that, in the Preisach model, the interaction field and switching fields are uncorrelated. However, in Figs. 5 and 6 the median point shifts to the left as one moves from the inner to the outer contours. This implies that the switching field and interaction field are correlated: a strong interaction is correlated with an effective decrease in the switching field. We suggest the median coercivity associated with the inner contours in Fig. 6 corresponds to the switching field of isolated particles, and that the median of the outer contours corresponds to an effective switching field of particles that occur in small clusters.

In most work on Preisach-type models, it is assumed that there is a Gaussian distribution of interaction fields, and that the switching field and interaction field distributions are uncorrelated. The above results indicate that these assumptions are invalid, at least in highly dispersed samples.

VI. COMPARISON WITH THE δM METHOD

Magnetic interactions can also be characterized using the δM method. The δM curve is calculated by comparing IRM and DCD curves, where the later starts at negative saturation. For a single domain, noninteracting system, the Wohlfarth equality[4] predicts that:

$$2*\mathrm{IRM}(H)/M_{\mathrm{rs}} = [1 + \mathrm{DCD}(H)/M_{\mathrm{rs}}]. \tag{11}$$

where M_{rs} is the saturation remanence. For a system of single domain particles, any deviation from equality can be attributed to interactions. δM is defined as the difference between the two sides of Eq. (11):

$$\delta M(H) = 2*\mathrm{IRM}(H)/M_{\mathrm{rs}} - 1 - \mathrm{DCD}(H)/M_{\mathrm{rs}}, \quad \text{where} \quad H \geqslant 0. \tag{12}$$

Hence, in the absence of interactions, δM will equal zero. When the δM curve falls entirely below the horizontal axis, a system is said to have negative interactions (i.e., the interactions destabilize the saturation remanence). When the δM curve lies above the horizontal axis, this indicates positive interactions. In cases where the curve crosses the horizontal axis, interpretation is more difficult. In practice, a small residual magnetization M_{re} can remain after demagnetization which can distort the results. Eq. (12) can be improved to account for the residual magnetization:

$$\delta M(H) = -1 - \mathrm{DCD}(H)/M_{\mathrm{rs}} + 2*\frac{[\mathrm{IRM}(H) - M_{\mathrm{re}}]/M_{\mathrm{rs}}}{(1 - M_{\mathrm{re}}/M_{\mathrm{rs}})}. \tag{13}$$

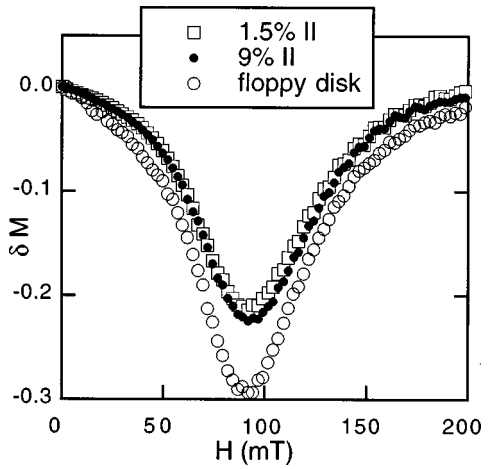

FIG. 11. δM curves for a typical floppy disk sample and the 1.5% and 9% Kodak samples, calculated with Eq. (13).

All of our samples produced negative interactions (Fig. 11). We let δM_p denote the magnitude of the negative peak of a $\delta M(H)$ curve, and used this as a measure of interaction strength. δM_p values for the Kodak samples (Table I) indicate increasing interactions with increasing concentration of magnetic particles, consistent with our ΔH_u measurements. However, ΔH_u gives a more precise measure of interactions than δM_p: the difference between δM_p values for the 9% II and 1.5% II Kodak samples is roughly $(0.231-0.214)=0.017$, whereas the separation between ΔH_u values is $(0.783-0.713)=0.070$. The standard deviations in the two types of measurement were determined by repeating each several times on a single sample, giving roughly 0.0012 for δM and 0.002 for ΔH_u. Dividing the above separations by the corresponding deviation gives $(0.017/0.0012)=14$ for the δM method, and $(0.07/0.002)=35$ for ΔH_u. The FORC method is therefore at least twice as sensitive in measuring interactions.

Precision is not the only advantage of the FORC method. On a FORC diagram, the effects of the interaction field mean and the interaction field variance are, at least to some approximation, decoupled. That is, the vertical displacement of the peak off the $H_u=0$ axis and the slope of the direction of contour elongation characterize the mean interaction field, while the vertical spread of the peak is a measure of the variance of the local interaction field. By contrast, it is not possible with a δM plot to decouple the effects of the mean interaction field from that of the local field variance. A system with a positive mean field and no local variance will have a positive δM curve; a system with a negative mean field will have a negative δM curve. But as Bertotti and Basso[12] and Basso *et al.*[13] have shown, variance in the local interaction field can also lead to a negative δM curve. They found that even when the mean interaction field is positive, a large enough variance can make the δM curve negative. This appears to be the case with our floppy disk sample: a FORC diagram (Fig. 2) indicates that this sample has a positive mean field and a large degree of local field variance. But on a δM curve, the variance dominates, and the curve is entirely negative (Fig. 11).

VII. CONCLUSIONS

We have demonstrated a practical technique for characterizing interacting single domain magnetic particle systems using FORC diagrams. The method has been tested on samples of highly dispersed particles and the results indicate that it provides a more precise measure of interaction strength than the more commonly used δM method. Furthermore, this method decouples the effects of the mean interaction field and local interaction field variance, which the δM method does not. For example, it was shown that a sample of typical floppy disk magnetic recording material, which has a negative δM curve, actually has a positive mean interaction field.

In addition, FORC diagrams can be used to obtain a more detailed understanding of magnetic interactions in highly dispersed particle systems than was previously possible. In particular, for the Kodak 1.5% sample, we find that there are two distinct populations of particles: a population of well-isolated particles and a population of small particle clusters. The switching field in the particle clusters was effectively reduced by interactions. FORC distributions therefore provide more detailed qualitative and quantitative information concerning magnetic particle assemblages than is available with other techniques.

ACKNOWLEDGMENTS

This work was supported by the University of Southampton Annual Grants Scheme and the Center for Statistics in Science and Technology at the University of California, Davis. The authors are grateful to Dr. Robert James of Eastman Kodak Company Research Laboratories, Rochester, NY, for supplying samples.

APPENDIX A: DISTINCTIONS BETWEEN FORC AND PREISACH DISTRIBUTIONS AND DIAGRAMS

A Preisach diagram is a contour plot of a Preisach distribution, which is used in a Preisach model of hysteresis. There are actually several variations of the Preisach model. In the basic Preisach model of an interacting single domain particle system, each particle is represented by a switching field and a local interaction field, where the local interaction field at each particle is assumed to be constant. A system of interacting particles is represented by a distribution of switching fields and interaction fields $P(H_{\mathrm{sw}},H_{\mathrm{int}})$, which is referred to as a Preisach distribution. The main objective in modeling a real particle system is to find the Preisach distribution such that the model gives the best possible agreement with that particular system's behavior.

Given a particular particle system, it might seem as though there should be a unique, precisely defined Preisach distribution to represent that system. This, however, is not the case. The fundamental problem is that the basic Preisach model does not have a rigorous physical basis. The assumption that there exists a constant, well-defined local interaction d at the site of each moment is not physically valid. The assumption that each particle has a well-defined switching field is also dubious, because the switching field of a particle will be effectively coupled to its interactions with surround-

ing particles, as discussed earlier. (These shortcomings are also shared by the more sophisticated versions of the Preisach model.) Because the basic Preisach model is not a rigorously valid physical model, the Preisach distribution used to describe a particular physical system will always be, to some degree, arbitrary. In fact, a number of different algorithms have been proposed in the literature for calculating Preisach distributions. In summary, a Preisach distribution is an ambiguously defined theoretical construction.

A FORC distribution, by contrast, is not based on any assumptions. It is not part of a theoretical model. It is simply a well-defined transform [i.e., Eq. (1)] of the set of first order reversal curves that is useful in making the structure of these data apparent to the human eye.

Furthermore, on physical grounds a symmetry condition is imposed upon any Preisach distribution: if an applied field history $H(t)$ gives a magnetization $M(t)$, then the opposite applied field history $-H(t)$ must give the opposite magnetization $-M(t)$. This requires that a Preisach distribution $P(H_{sw},H_{int})$ be symmetric about the $H_{int}=0$ axis, which corresponds to the $H_u=0$ axis on a FORC diagram. However, experimental FORC distributions are not, in general, symmetric about the $H_u=0$ axis (e.g., Fig. 2). This asymmetry can be corrected to some extent by incorporating a moving parameter into the calculations, as is done in the moving Preisach model.[11] But even with a moving parameter, some degree of asymmetry will almost always be present in an experimentally acquired FORC distribution. Hence, FORC distributions obtained from experimental data will not, in general, be valid Preisach distributions.

[1] X. He, C. Alexander, Jr., and M. R. Parker, IEEE Trans. Magn. **MAG-28**, 2683 (1992).
[2] R. Proksch and B. Moskowitz, J. Appl. Phys. **75**, 5894 (1994).
[3] P. Hejda, E. Petrovsky, and T. Zelinka, IEEE Trans. Magn. **MAG-30**, 896 (1994).
[4] E. P. Wohlfarth, J. Appl. Phys. **29**, 595 (1958).
[5] X.-D. Che and H. N. Bertram, J. Magn. Magn. Mater. **116**, 131 (1992).
[6] M. El-Hilo, K. O'Grady, P. I. Mayo, and R. W. Chantrell, IEEE Trans. Magn. **MAG-28**, 3282 (1992).
[7] I. D. Mayergoyz, IEEE Trans. Magn. **MAG-22**, 603 (1986).
[8] F. Preisach, Z. Phys. **94**, 277 (1935).
[9] P. J. Flanders, J. Appl. Phys. **63**, 3940 (1988).
[10] Logarithmic mean is defined as $\mu=\exp[\int_0^\infty dx\, f(x)\ln(x)]$ and logarithmic standard deviation is defined as $\sigma=\mathrm{sqrt}\{\int_0^\infty dx\, f(x)[\ln(x)-\ln(\mu)]^2\}$.
[11] F. Vajda and E. Torre, IEEE Trans. Magn. **MAG-27**, 4757 (1991).
[12] G. Bertotti and V. Basso, J. Appl. Phys. **73**, 5827 (1993).
[13] V. Basso, M. Lo Bue, and G. Bertotti, J. Appl. Phys. **75**, 5677 (1994).